BCL6 regulates brown adipocyte dormancy to maintain thermogenic reserve and fitness

Vassily I. Kutyavin[a] and Ajay Chawla[a,b,c,1,2]

[a]Cardiovascular Research Institute, University of California, San Francisco, CA 94143-0795; [b]Department of Physiology, University of California, San Francisco, CA 94143-0795; and [c]Department of Medicine, University of California, San Francisco, CA 94143-0795

Edited by Steven A. Kliewer, The University of Texas Southwestern Medical Center, Dallas, TX, and approved July 1, 2019 (received for review April 30, 2019)

Brown adipocytes provide a metabolic defense against environmental cold but become dormant as mammals habituate to warm environments. Although dormancy is a regulated response in brown adipocytes to environmental warmth, its transcriptional mechanisms and functional importance are unknown. Here, we identify B cell leukemia/lymphoma 6 (BCL6) as a critical regulator of dormancy in brown adipocytes but not for their commitment, differentiation, or cold-induced activation. In a temperature-dependent manner, BCL6 suppresses apoptosis, fatty acid storage, and coupled respiration to maintain thermogenic fitness during dormancy. Mechanistically, BCL6 remodels the epigenome of brown adipocytes to enforce brown and oppose white adipocyte cellular identity. Thus, unlike other thermogenic regulators, BCL6 is specifically required for maintaining thermogenic fitness when mammals acclimate to environmental warmth.

metabolism | transcription | thermogenesis | brown fat | acclimation

In mammals, brown and beige adipocytes generate heat (thermogenesis) through fuel oxidation and uncoupled respiration to defend core temperature in cold environments (1–4). As mammals acclimate to warm environments, their need for thermogenesis decreases, resulting in the entry of brown and beige adipocytes into a dormant state to conserve energy and prevent hyperthermia (1, 4). For example, depots of brown adipose tissue (BAT) in adult humans are largely dormant but can be activated by prolonged exposure to environmental cold or adrenergic agonists (5–9). Although entry of thermogenic adipocytes into dormancy is a well-appreciated adaptation to environmental warmth, the factors and mechanisms that regulate dormancy in BAT remain unknown.

While both brown and beige adipocytes undergo dormancy during acclimation to environmental warmth, their molecular, metabolic, and epigenetic states are quite distinct. For example, beige adipocytes lose virtually all of their thermogenic capacity during acclimation to environmental warmth, whereas brown adipocytes retain a significant portion of their thermogenic capacity even after remaining dormant for many weeks (10, 11). This distinction between beige and brown adipocytes is also observed at the level of the epigenome. For example, the enhancer landscape of beige adipocytes undergoes profound remodeling during adaptation to warmth, becoming almost indistinguishable from that of white adipocytes (10). In contrast, brown adipocytes largely maintain their chromatin state during dormancy, which allows them to maintain their thermogenic capacity (10). However, it is not known what factors contribute to maintenance of a stable epigenetic state during brown adipocyte dormancy.

B cell leukemia/lymphoma 6 (BCL6), a sequence-specific transcriptional repressor, is expressed in many cell types but has been best studied in the immune system. In germinal center B cells, it plays an essential role in the germinal center reaction by repressing genes involved in DNA damage response, apoptosis, cell activation, and plasma cell differentiation (12, 13). BCL6 is also required for the differentiation of follicular helper T cells and modulates the inflammatory activation of macrophages (14–17). Outside the immune system, BCL6 is expressed in metabolic tissues, such as adipocytes and liver, where its functions are just beginning to be investigated (18–22). For example, a recent report found that deletion of *Bcl6* in all adipocytes increased de novo lipogenesis, resulting in selective expansion of subcutaneous white adipose tissue (WAT) and protection from obesity-induced insulin resistance (21). Although these studies suggest a potential role for BCL6 in fatty acid metabolism, the role of BCL6 in brown adipocyte biology has not been explored.

Here, we investigated the regulatory functions of BCL6 in both metabolically active and dormant brown adipocytes. We found that loss of BCL6 did not impair the commitment, differentiation, or adrenergic activation of brown adipocytes, but it selectively impaired their thermogenic capacity during dormancy. Thus, unlike other thermogenic regulators that act downstream of the sympathetic nervous system, our data suggest that BCL6 acts in parallel with the sympathetic nervous system to reinforce brown adipocyte cellular identity during dormancy.

Results

BCL6 Maintains Thermogenic Capacity of BAT during Dormancy. BCL6 is expressed in mature BAT and differentiating brown adipocytes (*SI Appendix*, Fig. S1 *A* and *B*), where its functions are not well

Significance

During exposure to environmental cold, brown adipocytes protect against hypothermia by generating heat (thermogenesis). In warm environments, brown adipocytes become inactive or dormant but still maintain their identity and thermogenic capacity, allowing rapid reactivation of thermogenesis upon subsequent cold exposure. Our understanding of the dormant state and its regulation is very limited. Here, we show that the transcription factor B cell leukemia/lymphoma 6 (BCL6) is specifically required for maintenance of thermogenic capacity during dormancy in brown adipocytes. Mechanistically, BCL6 drives a gene expression program that promotes survival, fatty acid oxidation, and uncoupled respiration. Thus, unlike other transcription factors that regulate cold-induced thermogenesis, BCL6 is specifically required for maintaining thermogenic fitness during adaptation to environmental warmth.

Author contributions: V.I.K. and A.C. designed research; V.I.K. performed research; V.I.K. and A.C. analyzed data; and V.I.K. and A.C. wrote the paper.

The authors declare no conflict of interest.

This article is a PNAS Direct Submission.

Data deposition: The data reported in this paper have been deposited in the Gene Expression Omnibus (GEO) database, https://www.ncbi.nlm.nih.gov/geo (accession no. GSE122746).

[1]To whom correspondence may be addressed. Email: Ajay.Chawla@ucsf.edu.

[2]Present address: Merck Research Labs, SAF-803, South San Francisco, CA 94080.

This article contains supporting information online at www.pnas.org/lookup/suppl/doi:10.1073/pnas.1907308116/-/DCSupplemental.

Published online August 2, 2019.

understood. To investigate the role of BCL6 in brown adipocyte biology, we crossed *Bcl6*$^{f/f}$ mice on C57BL6/J background with *Ucp1*^{Cre}, *Adipoq*^{Cre}, and *Myf5*^{Cre} to generate conditional knockouts of BCL6 in BAT (*Bcl6*$^{f/f}$*Ucp1*^{Cre}), pan-adipose (*Bcl6*$^{f/f}$*Adipoq*^{Cre}), and Myf5^{+} somitic brown adipocyte precursors (*Bcl6*$^{f/f}$*Myf5*^{Cre}), respectively (Fig. 1*A*). In contrast to a previous study that implicated BCL6 in commitment and differentiation of adipocyte precursors (20), we found that BCL6 was not required in Myf5^{+} precursors for the development of the brown adipocyte lineage (Fig. 1*B*). Furthermore, in mice raised at the normal vivarium temperature of 22 °C, BCL6 was not required for cold-induced thermogenesis, as evidenced by normal core body temperature and survival of *Bcl6*$^{f/f}$*Ucp1*^{Cre} and *Bcl6*$^{f/f}$*Adipoq*^{Cre} mice upon acute exposure to 4 °C (Fig. 1 *C* and *D* and *SI Appendix*, Fig. S1*C*). Since BCL6 was not required for BAT thermogenesis in cold-adapted mice (i.e., raised at 22 °C), we considered the alternative hypothesis that BCL6 is important for maintenance of thermogenic capacity in dormant BAT.

To investigate the role of BCL6 in BAT dormancy, we bred and reared mice at thermoneutrality (30 °C), a warm environment that minimizes thermogenesis and promotes entry of BAT into its dormant state. Although thermoneutral housing did not alter expression of the BCL6 protein in BAT (*SI Appendix*, Fig. S1*D*), loss of BCL6 had a profound effect on the thermogenic competence of dormant BAT. For example, during a cold challenge from 30 °C to 10 °C, core temperature rapidly declined in *Bcl6*$^{f/f}$*Ucp1*^{Cre} and *Bcl6*$^{f/f}$*Myf5*^{Cre} mice, resulting in severe hypothermia (Fig. 1*E* and *SI Appendix*, Fig. S1*E*). In both conditional knockouts, the inability to maintain core temperature was uniformly lethal, whereas the majority of the control animals were able to survive the cold challenge after adaptation to thermoneutrality (Fig. 1*F* and *SI Appendix*, Fig. S1*F*).

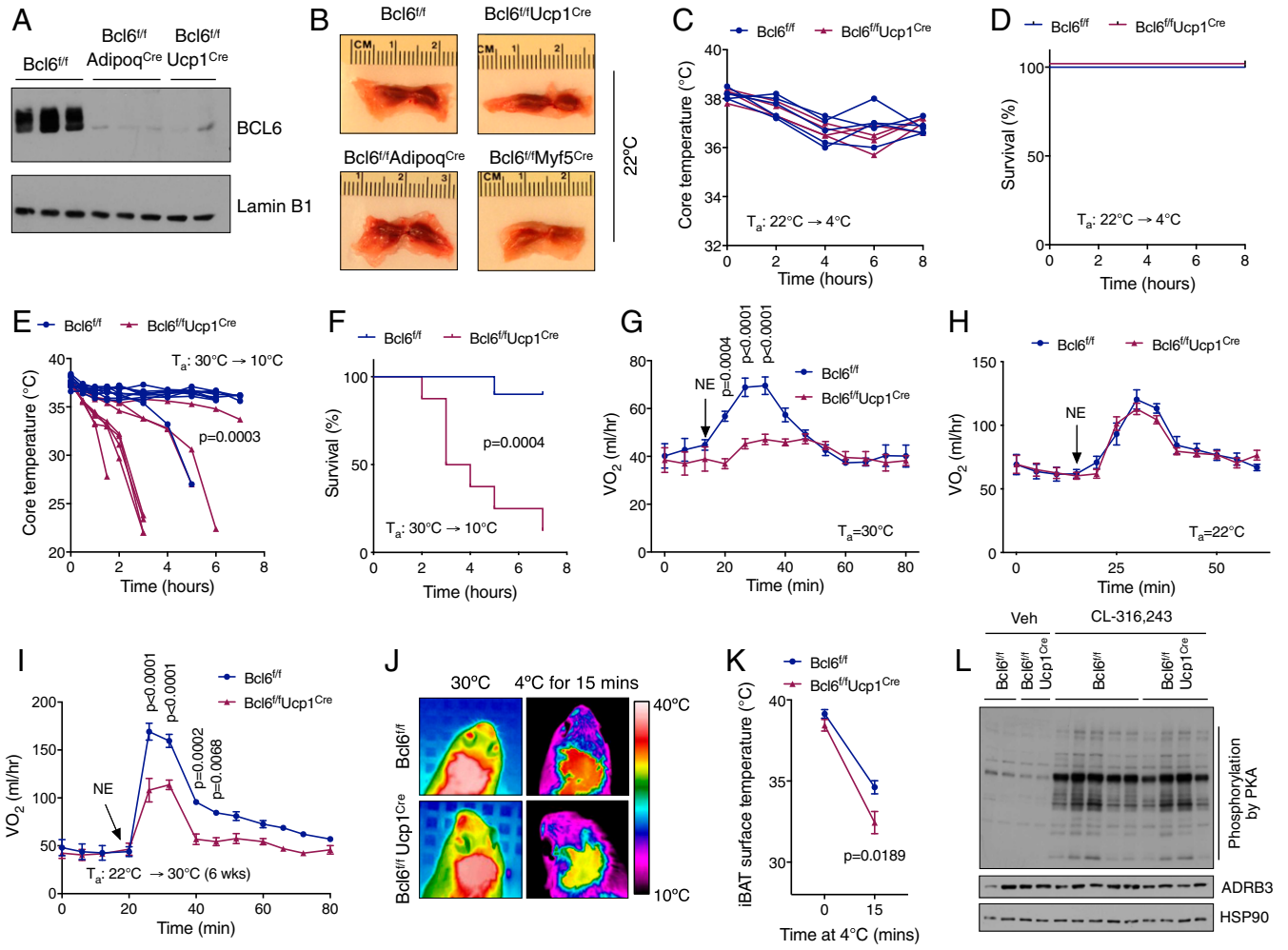

Fig. 1. BCL6 is required to maintain thermogenic capacity of dormant BAT. (*A*) Immunoblotting for BCL6 and lamin B1 protein in nuclear extracts of iBAT of *Bcl6*$^{f/f}$, *Bcl6*$^{f/f}$*Ucp1*^{Cre}, and *Bcl6*$^{f/f}$*Adipoq*^{Cre} mice ($n = 2$ to 3 per genotype). (*B*) Gross morphology of iBAT isolated from *Bcl6*$^{f/f}$, *Bcl6*$^{f/f}$*Ucp1*^{Cre}, *Bcl6*$^{f/f}$*Adipoq*^{Cre}, and *Bcl6*$^{f/f}$*Myf5*^{Cre} mice bred and housed at 22 °C. (*C* and *D*) Core temperature measurements (*C*) and survival curves (*D*) of *Bcl6*$^{f/f}$ and *Bcl6*$^{f/f}$*Ucp1*^{Cre} female mice bred at 22 °C and subjected to 4 °C cold challenge ($n = 4$ to 5 per genotype). (*E* and *F*) Core temperature measurements (*E*) and survival curves (*F*) of *Bcl6*$^{f/f}$ and *Bcl6*$^{f/f}$*Ucp1*^{Cre} female mice bred at 30 °C and subjected to 10 °C cold challenge ($n = 8$ to 10 per genotype). The *P* value for *E* was calculated using the Mann–Whitney *U* test at the 3 h time point. (*G* and *H*) Norepinephrine-stimulated changes in oxygen consumption rate (VO_2) in *Bcl6*$^{f/f}$ and *Bcl6*$^{f/f}$*Ucp1*^{Cre} female mice housed at 30 °C (*G*, $n = 6$ per genotype) or 22 °C (*H*, $n = 4$ to 6 per genotype). The arrow indicates the time of norepinephrine (NE) injection. (*I*) Norepinephrine-stimulated changes in oxygen consumption rate (VO_2) in *Bcl6*$^{f/f}$ and *Bcl6*$^{f/f}$*Ucp1*^{Cre} male mice initially housed at 22 °C (until 5 wk of age) followed by housing at 30 °C for 6 wk ($n = 3$ to 5 per genotype). (*J* and *K*) Representative infrared images (*J*) and quantified thermographic measurements of interscapular surface temperature (*K*) for *Bcl6*$^{f/f}$ and *Bcl6*$^{f/f}$*Ucp1*^{Cre} male mice subjected to 4 °C cold challenge from 30 °C ($n = 5$ to 6 per genotype). (*L*) Immunoblotting for phosphorylated PKA substrates, β3-adrenergic receptor (ADRB3), and HSP90 in whole-cell extracts of iBAT of *Bcl6*$^{f/f}$ and *Bcl6*$^{f/f}$*Ucp1*^{Cre} male mice that were housed at 30 °C and injected with CL-316,243 (1 mg/kg) or vehicle (Veh) for 30 min. Data are presented as mean ± SEM.

We next asked whether a decrease in thermogenic capacity of dormant BAT led to cold intolerance in *Bcl6*$^{f/f}$*Ucp1*^{Cre} mice. Using norepinephrine-stimulated whole-body oxygen consumption, which reflects the organism's thermogenic capacity (23, 24), we found that *Bcl6*$^{f/f}$*Ucp1*^{Cre} mice had a blunted rise in the rate of oxygen consumption when they were bred or adapted at 30 °C but not at 22 °C (Fig. 1 *G*–*I*). In agreement with these data, thermographic imaging revealed lower surface temperature over interscapular BAT (iBAT) in 30 °C-adapted *Bcl6*$^{f/f}$*Ucp1*^{Cre} and *Bcl6*$^{f/f}$*Adipoq*^{Cre} mice during an acute cold challenge (Fig. 1 *J* and *K* and *SI Appendix*, Fig. S1*G*), which contributed to lethal hypothermia and impaired survival in 30 °C-adapted *Bcl6*$^{f/f}$*Adipoq*^{Cre} mice (*SI Appendix*, Fig. S1 *H* and *I*). This decrease in thermogenesis by iBAT of *Bcl6*$^{f/f}$*Ucp1*^{Cre} mice could not be accounted for by changes in adrenergic signaling because expression of β3-adrenergic receptor and PKA-dependent phosphorylation in response to β3-adrenergic agonist CL-316,243 were preserved in iBAT of *Bcl6*$^{f/f}$*Ucp1*^{Cre} mice (Fig. 1*L*). Together, these findings demonstrate that BCL6 is specifically required for the maintenance of thermogenic capacity in dormant (adapted to 30 °C) but not active iBAT (adapted to 22 °C).

BCL6 Maintains Uncoupled Respiration in Dormant BAT. We next asked whether loss of BCL6 affected respiratory capacity of dormant BAT. We found that after an acute cold challenge, oxygen consumption in isolated iBAT was reduced by ∼40 to 50% in *Bcl6*$^{f/f}$*Ucp1*^{Cre} and *Bcl6*$^{f/f}$*Adipoq*^{Cre} mice adapted to environmental warmth (Fig. 2*A* and *SI Appendix*, Fig. S2*A*). A similar result was observed for isolated iBAT mitochondria (*SI Appendix*, Fig. S2*B*). This decrease in mitochondrial respiration was associated with nearly complete absence of UCP1 mRNA and protein in iBAT of warm-adapted (30 °C), but not cold-adapted (22 °C), *Bcl6*$^{f/f}$*Ucp1*^{Cre} mice (Fig. 2*B* and *SI Appendix*, Fig. S2*C*). A similar decrease in UCP1 protein expression was also observed when *Bcl6*$^{f/f}$*Ucp1*^{Cre} mice that were bred at 22 °C were adapted to 30 °C for 6 wk, independently verifying the importance of BCL6 in regulation of

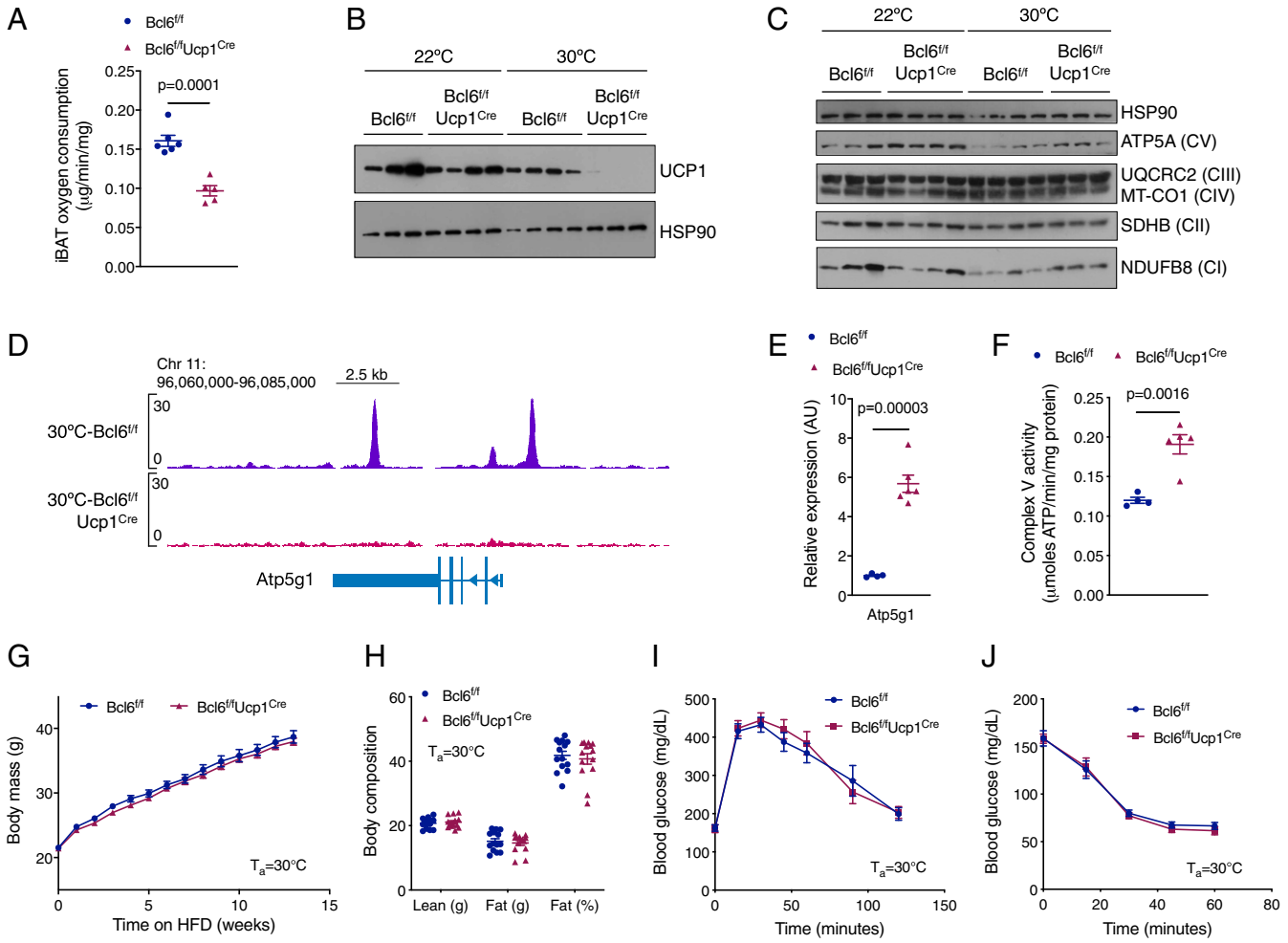

Fig. 2. BCL6 maintains uncoupled respiration in dormant BAT. (*A*) Oxygen consumption rate of iBAT isolated from *Bcl6*$^{f/f}$ and *Bcl6*$^{f/f}$*Ucp1*^{Cre} mice housed at 30 °C and exposed to 4 °C for 15 min ($n = 5$ to 6 per genotype). (*B*) Immunoblotting for UCP1 and HSP90 in whole-cell extracts of iBAT of male 8-wk-old mice housed at 22 °C or 30 °C ($n = 3$ to 4 per genotype and temperature). (*C*) Immunoblotting for subunits of mitochondrial complexes I to V and HSP90 in iBAT of *Bcl6*$^{f/f}$ and *Bcl6*$^{f/f}$*Ucp1*^{Cre} mice housed at 22 °C or 30 °C ($n = 3$ to 4 per genotype and temperature). (*D*) Genome browser track showing BCL6 binding near the promoter of the *Atp5g1* gene in iBAT isolated from *Bcl6*$^{f/f}$ and *Bcl6*$^{f/f}$*Ucp1*^{Cre} (negative control) mice housed at 30 °C. Kb, kilobases. (*E*) Quantitative RT-PCR measurement of *Atp5g1* mRNA in iBAT of *Bcl6*$^{f/f}$ and *Bcl6*$^{f/f}$*Ucp1*^{Cre} mice housed at 30 °C ($n = 4$ to 6 per genotype). AU, arbitrary units. (*F*) ATP synthase activity in mitochondria isolated from iBAT of *Bcl6*$^{f/f}$ and *Bcl6*$^{f/f}$*Ucp1*^{Cre} mice housed at 30 °C ($n = 4$ to 5 per genotype). (*G*) Body mass of male *Bcl6*$^{f/f}$ and *Bcl6*$^{f/f}$*Ucp1*^{Cre} mice fed a high-fat diet at 30 °C starting at the age of 10 wk ($n = 13$ per genotype, data pooled from multiple experiments). (*H*) Body composition analysis by dual-energy X-ray absorptiometry (DEXA) of male *Bcl6*$^{f/f}$ and *Bcl6*$^{f/f}$*Ucp1*^{Cre} mice fed a high-fat diet at 30 °C ($n = 14$ per genotype, data pooled from multiple experiments). (*I* and *J*) Glucose (*I*) and insulin (*J*) tolerance tests in male *Bcl6*$^{f/f}$ and *Bcl6*$^{f/f}$*Ucp1*^{Cre} mice fed a high-fat diet at 30 °C ($n = 14$ to 15 per genotype, data pooled from multiple experiments). Data are presented as mean ± SEM.

BAT dormancy (*SI Appendix*, Fig. S2*D*). In contrast, mitochondrial abundance, cristae density, expression of respiratory chain complexes I to IV, and complex I activity were not significantly different between dormant iBAT of $Bcl6^{f/f}$ and $Bcl6^{f/f}Ucp1^{Cre}$ mice (Fig. 2*C* and *SI Appendix*, Fig. S2 *E–I*).

Because we observed that expression of ATP5A, an F_1 subunit of ATP synthase, was increased in iBAT of $Bcl6^{f/f}Ucp1^{Cre}$ mice (Fig. 2*C*), we hypothesized that BCL6 might regulate switching between uncoupled (UCP1-mediated) and coupled (ATP synthase–mediated) respiration. Chromatin immunoprecipitation followed by sequencing (ChIP-seq) analysis (described below) revealed BCL6 binding sites near the promoter region of the *Atp5g1* gene (Fig. 2*D*), which encodes the rate-limiting component in the assembly of ATP synthase in brown adipocytes (25, 26). Consistent with our hypothesis, loss of BCL6 resulted in increased expression of *Atp5g1* mRNA, resulting in higher ATP synthase activity in dormant iBAT of $Bcl6^{f/f}Ucp1^{Cre}$ mice (Fig. 2 *E* and *F*). These findings suggest that BCL6 suppresses coupled respiration while maintaining uncoupled respiration in BAT during dormancy.

In addition to cold-induced thermogenesis, previous studies have implicated UCP1 in diet-induced thermogenesis, which can mitigate the deleterious effects of high-fat diet (HFD) feeding (27). These observations prompted us to ask whether BCL6 in brown adipocytes might also regulate diet-induced thermogenesis. To test this hypothesis, we housed $Bcl6^{f/f}$ and $Bcl6^{f/f}Ucp1^{Cre}$ mice at thermoneutrality (30 °C) and fed them HFD for 13 wk. We found that body mass, body composition, glucose tolerance, and insulin sensitivity were not significantly different between the 2 genotypes after HFD feeding (Fig. 2 *G–J*). Similar results were obtained in $Bcl6^{f/f}Adipoq^{Cre}$ mice that were fed HFD at thermoneutrality (*SI Appendix*, Fig. S3 *A–E*). In aggregate, these results suggest that while BCL6 is required for the maintenance of BAT's thermogenic capacity during dormancy, it is dispensable for diet-induced thermogenesis.

BCL6 Regulates Survival of Dormant Brown Adipocytes. To further investigate the molecular basis for how BCL6 regulates thermogenic capacity in dormant brown adipocytes, we analyzed the iBAT transcriptome of $Bcl6^{f/f}$ and $Bcl6^{f/f}Ucp1^{Cre}$ mice that were cold (22 °C) or warm (30 °C) adapted using RNA-seq. This analysis revealed that BCL6 regulates the iBAT transcriptome in a temperature-dependent manner. For example, ∼42 and ∼52% of all induced and repressed genes, respectively, were only significantly altered at 30 °C (Fig. 3*A*). Because BCL6 functions as a transcriptional repressor in other contexts, we first focused on genes induced in iBAT of $Bcl6^{f/f}Ucp1^{Cre}$ mice. Gene ontology enrichment analysis revealed significant enrichment of immune, inflammatory, and apoptotic processes (Fig. 3*B*). For instance, a large group of genes involved in extrinsic and intrinsic pathways of apoptosis, including *Bcl10*, *Bmf*, *Traf1*, *Dlc1*, *Litaf*, *Tnfrsf10b*, *Dapk1*, *Wdr92*, and *Egln3*, was induced in iBAT of $Bcl6^{f/f}Ucp1^{Cre}$ mice housed at 30 °C (Fig. 3*C* and *SI Appendix*, Table S1). While many of these genes were also up-regulated at 22 °C, their induction was much lower at 22 °C (Fig. 3*C*), indicating a greater dependence on BCL6 for their repression during dormancy at 30 °C. A gene signature of tissue inflammation was also induced in iBAT of warm-adapted (30 °C) $Bcl6^{f/f}Ucp1^{Cre}$ mice (*SI Appendix*, Fig. S4*A* and Table S2); however, flow cytometric analysis did not reveal increased recruitment of immune cells into iBAT, indicating the absence of an overt inflammatory response (*SI Appendix*, Fig. S4 *B–D*).

We next asked whether the induced genes were direct targets of BCL6 in brown adipocytes. ChIP-seq revealed 3,022 binding sites for BCL6 in dormant BAT, which localized primarily to intronic, intergenic, and promoter regions (Fig. 3*D*). De novo motif analysis revealed enrichment for the consensus BCL6 binding motif among the identified peaks (*SI Appendix*, Fig. S4*E*), confirming the specificity of the ChIP-seq. We next asked whether the genes closest to the BCL6 binding sites were differentially expressed in iBAT of $Bcl6^{f/f}Ucp1^{Cre}$ mice. Using a fold change threshold of >1.5 and a false discovery rate threshold of <0.05, we identified 112 and 226 genes that exhibited positive and negative dependence on BCL6, respectively, for their expression in iBAT (Fig. 3*E* and *SI Appendix*, Table S3). Among these genes, we found specific binding of BCL6 near proapoptotic genes *Bmf*, *Egln3*, *Dapk1*, and *Wdr92* (Fig. 3*F* and *SI Appendix*, Table S3), whose expression was induced in dormant iBAT of $Bcl6^{f/f}Ucp1^{Cre}$ mice (Fig. 3*G*). Taken together, these data indicate that BCL6 represses expression of proapoptotic genes in brown adipocytes, which might enhance their survival during dormancy.

Previous studies have demonstrated that in addition to activating thermogenesis, adrenergic stimuli promote survival of brown adipocytes (28, 29). This led us to ask whether BCL6 might function in parallel with sympathetic signaling to promote survival of brown adipocytes during dormancy. In support of this hypothesis, we observed a higher frequency of apoptotic cells in dormant iBAT of $Bcl6^{f/f}Ucp1^{Cre}$ mice, which over time resulted in reduced BAT mass and DNA content in the adipocyte fraction (Fig. 3 *H–J* and *SI Appendix*, Fig. S4*F*). In contrast, during housing at 22 °C, the frequency of apoptotic cells was not increased, and BAT mass was not reduced in $Bcl6^{f/f}Ucp1^{Cre}$ mice (Fig. 3 *H* and *I*). Because the frequency of $Ki67^{+}$ proliferating cells was not significantly different between the genotypes (*SI Appendix*, Fig. S4 *G* and *H*), these data suggest that BCL6 promotes survival of brown adipocytes specifically during dormancy, when sympathetic input into BAT is minimal.

BCL6 Regulates Fatty Acid Metabolism in Dormant BAT. We next turned our attention to the genes that are down-regulated in dormant iBAT of $Bcl6^{f/f}Ucp1^{Cre}$ mice. Gene ontology enrichment analysis of down-regulated genes revealed significant enrichment of fatty acid β-oxidation, tricarboxylic acid (TCA) cycle, and carbohydrate metabolism processes in iBAT of warm-adapted (30 °C) $Bcl6^{f/f}Ucp1^{Cre}$ mice (Fig. 4*A*). For example, we observed that almost the entire program for β-oxidation of fatty acids was suppressed in dormant iBAT of $Bcl6^{f/f}Ucp1^{Cre}$ mice (Fig. 4*B*). While a similar trend was observed at 22 °C, the magnitude of change was lower (Fig. 4*B*), indicating greater dependence on BCL6 in the dormant state (30 °C). This decrease in catabolism of fatty acids was accompanied by induction of acyl-CoA thioesterases (ACOTs), enzymes that hydrolyze fatty acyl-CoAs to the metabolically inactive fatty acid form (30). In particular, we observed that many of the cytosolic and peroxisomal ACOTs (*Acot1, Acot3, Acot4, Acot7,* and *Acot8*) were induced in iBAT of $Bcl6^{f/f}Ucp1^{Cre}$ mice during dormancy, whereas expression of mitochondrial ACOTs (*Acot2, Acot9, Acot13,* and *Them4*) was more variable (Fig. 4*C*). In contrast, the expression of acyl-CoA synthetases, which catalyze the reverse reaction of synthesizing acyl-CoAs from fatty acids, was not significantly different between the genotypes (*SI Appendix*, Fig. S5*A*).

The importance of ACOTs in fatty acid metabolism prompted us to take a closer look at the regulation of these genes by BCL6. While ChIP-seq revealed that BCL6 bound near the promoter region of *Acot1* (Fig. 4*D*), expression of *Acot1*, as well as the neighboring *Acot3* and *Acot4* genes, was increased in dormant iBAT of $Bcl6^{f/f}Ucp1^{Cre}$ mice (Fig. 4*E*), indicating potential coregulation of these ACOT genes by BCL6. Because shifts in ACOT activity can alter the balance between oxidation and storage of fatty acids (30, 31), we next quantified ACOT activity in iBAT. We found that ACOT activity was increased by ∼40% in the cytosolic but not the mitochondrial fraction of iBAT isolated from warm-adapted (30 °C) $Bcl6^{f/f}Ucp1^{Cre}$ mice (Fig. 4 *F* and *G*). These data together suggest a model in which BCL6 determines how fatty acids are apportioned between storage and oxidation in brown

adipocytes. In the absence of BCL6, activation and oxidation of fatty acids is decreased, favoring their storage into cytosolic lipid droplets (Fig. 4 *H* and *I* and *SI Appendix*, Fig. S5 *B* and *C*).

BCL6 Reinforces Brown- and Opposes White-Specific Enhancers to Maintain Cellular Identity. Because genes involved in thermogenic metabolism were suppressed in dormant BAT of *Bcl6*$^{f/f}$*Ucp1*^{Cre} mice, we asked whether this represented a shift in brown adipocyte cellular state or identity. Analysis of the BATLAS gene set, which can robustly differentiate between brown and white adipocytes (32), revealed that loss of BCL6 led to up-regulation of white adipocyte (such as *Lep*, *Nnat*, *Igf1*, *Ccdc80*, and *Gadd45a*) and down-regulation of brown adipocyte (such as *Acads*, *Cpt1b*, *Ech1*, *Hadha*, *Idh3a*, *Ndufs1*, *Sdha*, *Suclg1*, and *Ucp1*) markers in dormant iBAT of *Bcl6*$^{f/f}$*Ucp1*^{Cre} mice (Fig. 5*A* and *SI Appendix*, Table S4). These changes in gene expression suggested that BCL6 might regulate brown adipocyte cellular identity during dormancy by maintaining a stable chromatin state. To test this hypothesis, we used ChIP-seq to measure the genome-wide abundance of acetylated histone 3 lysine 27 (H3K27ac), which marks active enhancers and promoters. We found that deletion of *Bcl6* altered the chromatin state of brown adipocytes in a temperature-dependent manner. For example, H3K27 acetylation was increased at 224 sites and reduced at 1,011 sites in iBAT of warm-adapted *Bcl6*$^{f/f}$*Ucp1*^{Cre} mice (Fig. 5*B* and *SI Appendix*, Fig. S6*A*), whereas acetylation was increased at 303 sites but reduced at only 228 sites in iBAT of cold-adapted *Bcl6*$^{f/f}$*Ucp1*^{Cre} mice (*SI Appendix*, Fig. S6 *A* and *B*).

We next asked whether these global changes in the chromatin state of *Bcl6*$^{f/f}$*Ucp1*^{Cre} mice reflected a shift in adipocyte lineage-specific enhancers. For this analysis, we first constructed a list of brown

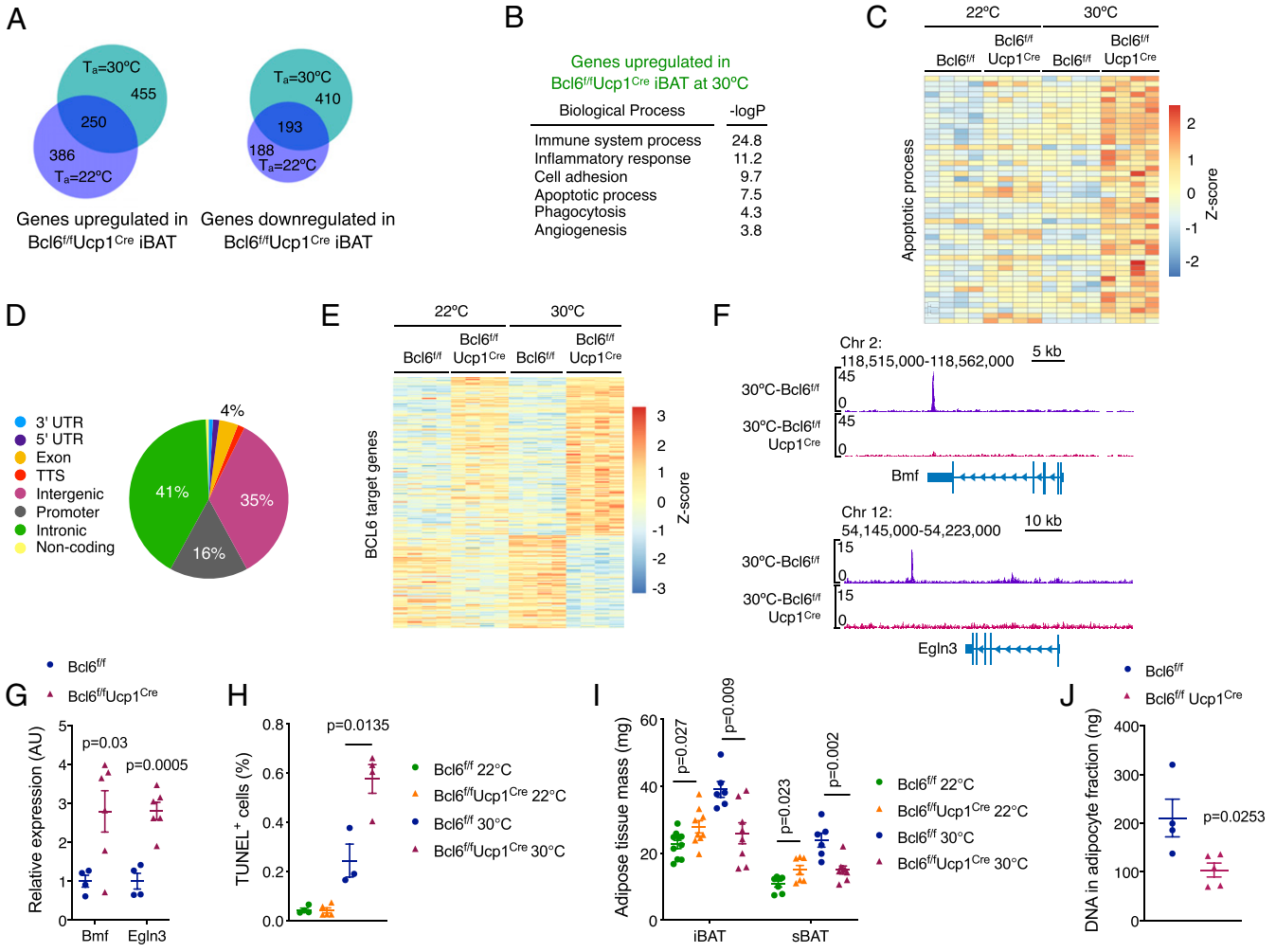

Fig. 3. BCL6 regulates survival of dormant brown adipocytes. (*A*) Venn diagrams showing differentially expressed genes in iBAT of *Bcl6*$^{f/f}$*Ucp1*^{Cre} mice (fold change ≥ 1.5, adjusted *P* value < 0.05). Genes up-regulated (*Left*) and down-regulated (*Right*) in iBAT of *Bcl6*$^{f/f}$*Ucp1*^{Cre} mice that were housed at different ambient temperatures. (*B*) Gene ontology enrichment analysis of up-regulated genes in iBAT of *Bcl6*$^{f/f}$*Ucp1*^{Cre} mice housed at 30 °C. Enriched biological processes and corresponding *P* values are shown. (*C*) Heat map of up-regulated genes in the "apoptotic process" gene ontology category in iBAT of *Bcl6*$^{f/f}$ and *Bcl6*$^{f/f}$*Ucp1*^{Cre} mice ($n = 4$ per genotype and temperature). The list of genes is provided in *SI Appendix*, Table S1. (*D*) Pie chart showing the distribution of BCL6 binding sites across the genome of iBAT. TTS, transcription termination site. (*E*) Heat map of BCL6-regulated genes (fold change ≥1.5) in iBAT of *Bcl6*$^{f/f}$ and *Bcl6*$^{f/f}$*Ucp1*^{Cre} mice housed at 30 °C that are nearest to a BCL6 binding site. The list of genes is provided in *SI Appendix*, Table S3. (*F*) Genome browser tracks showing BCL6 binding sites near proapoptotic genes *Bmf* and *Egln3* in iBAT isolated from *Bcl6*$^{f/f}$ and *Bcl6*$^{f/f}$*Ucp1*^{Cre} (negative control) mice housed at 30 °C. (*G*) Quantitative RT-PCR measurement of *Bmf* and *Egln3* mRNAs in iBAT of *Bcl6*$^{f/f}$ and *Bcl6*$^{f/f}$*Ucp1*^{Cre} mice housed at 30 °C ($n = 4$ to 6 per genotype). (*H*) Quantification of terminal deoxynucleotidyl transferase dUTP nick end labeled (TUNEL^{+}) apoptotic cells in iBAT of *Bcl6*$^{f/f}$ and *Bcl6*$^{f/f}$*Ucp1*^{Cre} male mice housed at 22 °C or 30 °C for 1 wk ($n = 3$ to 5 per genotype). (*I*) BAT mass in 8-wk-old *Bcl6*$^{f/f}$ and *Bcl6*$^{f/f}$*Ucp1*^{Cre} male mice bred at 22 °C or 30 °C ($n = 6$ to 10 per genotype and condition). sBAT = subscapular BAT. (*J*) DNA content in adipocyte fraction of iBAT from *Bcl6*$^{f/f}$ and *Bcl6*$^{f/f}$*Ucp1*^{Cre} mice bred at 30 °C ($n = 4$ to 5 per genotype). Data are presented as mean ± SEM.

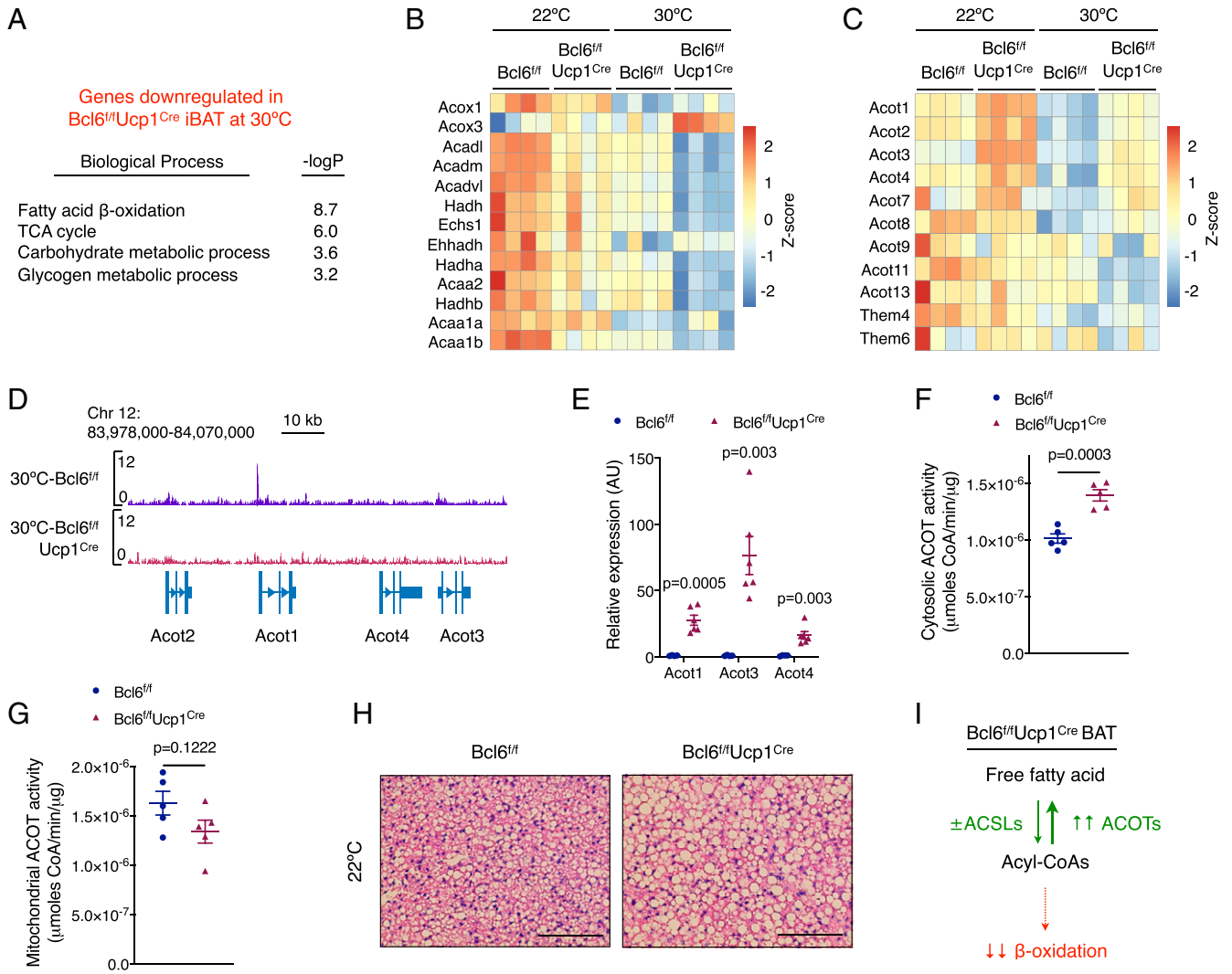

Fig. 4. BCL6 regulates fatty acid metabolism in dormant BAT. (*A*) Gene ontology enrichment analysis and corresponding *P* values for the down-regulated genes in iBAT of *Bcl6$^{f/f}$Ucp1^{Cre}* mice housed at 30 °C. (*B* and *C*) Heat maps of genes involved in β-oxidation of fatty acids (*B*) and acyl-CoA thioesterase (ACOT) genes (*C*) ($n = 4$ per genotype and temperature). (*D*) Genome browser track showing BCL6 binding site near the promoter of *Acot1* gene in iBAT isolated from *Bcl6$^{f/f}$* and *Bcl6$^{f/f}$Ucp1^{Cre}* (negative control) mice housed at 30 °C. (*E*) Quantitative RT-PCR measurement of *Acot1*, *Acot3*, and *Acot4* mRNAs in iBAT of *Bcl6$^{f/f}$* and *Bcl6$^{f/f}$Ucp1^{Cre}* mice housed at 30 °C ($n = 4$ to 6 per genotype). (*F* and *G*) Measurement of ACOT activity in cytosolic (*F*) and mitochondrial (*G*) fractions of isolated iBAT of *Bcl6$^{f/f}$* and *Bcl6$^{f/f}$Ucp1^{Cre}* mice housed at 30 °C ($n = 5$ per genotype). ACOT activity is expressed as micromoles of CoA produced per minute per microgram of protein. (*H*) Hematoxylin and eosin staining of representative iBAT sections from *Bcl6$^{f/f}$* and *Bcl6$^{f/f}$Ucp1^{Cre}* mice bred and housed at 22 °C. (Scale bar, 100 μm.) (*I*) A model depicting changes in fatty acid metabolism in dormant BAT of *Bcl6$^{f/f}$Ucp1^{Cre}* mice. Data are presented as mean ± SEM.

and white adipocyte–specific enhancers (enriched more than 4-fold in either brown or white adipocytes) from the previously identified group of adipocyte enhancers (10, 33) (*SI Appendix*, Dataset S1). We then asked how loss of BCL6 affected the activation of these enhancers in dormant iBAT. We found that approximately half (~55%) of BCL6-dependent enhancers were brown or white adipocyte–specific enhancers (Fig. 5*C*). Importantly, the direction of regulation by BCL6 at these enhancers clearly indicated a critical role for BCL6 in reinforcement of brown adipocyte cellular identity. For example, among the BCL6-regulated brown adipocyte–specific enhancers, 99% exhibited decreased acetylation in *Bcl6$^{f/f}$Ucp1^{Cre}* iBAT (Fig. 5*D*). In contrast, 100% of the BCL6-regulated white adipocyte–specific enhancers exhibited increased acetylation in the *Bcl6$^{f/f}$Ucp1^{Cre}* iBAT (Fig. 5*E*). Although the number of BCL6-dependent active enhancers was about 2-fold lower in iBAT of cold-adapted mice (*SI Appendix*, Fig. S6*C*), BCL6 acted in a similar manner at these enhancers (*SI Appendix*, Fig. S6 *D* and *E*). In particular, we found that H3K27 acetylation was reduced at brown adipocyte–specific enhancers associated with *Ucp1*, *Elovl3*, *Acaa1b*, *Cidea*, *Slc27a2*, *Gdf*, and *Ptk2b* (Fig. 5*F* and *SI Appendix*, Fig. S6*F*). In contrast, we found that H3K27 acetylation was increased at white adipocyte–specific enhancers associated with *Ccdc80*, *Lep*, and *Nnat* in iBAT of *Bcl6$^{f/f}$Ucp1^{Cre}* mice (Fig. 5*G* and *SI Appendix*, Fig. S6*G*). Similar enrichment of H3K27 acetylation was observed near BCL6 target genes in iBAT of *Bcl6$^{f/f}$Ucp1^{Cre}* mice, including *Atp5g1*, acyl-CoA thioesterases (*Acot1*, *Acot3*, and *Acot4*), and *Bmf* (Fig. 5 *F* and *G*, and *SI Appendix*, Fig. S6*H*), consistent with their direct repression by BCL6. In aggregate, these results indicate that BCL6 maintains thermogenic capacity of dormant BAT in part by reinforcing brown adipocyte–specific enhancers while concurrently suppressing white adipocyte–specific enhancers.

BCL6 Regulates Brown Adipocyte Enhancers by Direct and Indirect Mechanisms. Because BCL6 binding sites were not identified near the majority of altered enhancers in the iBAT of *Bcl6$^{f/f}$Ucp1^{Cre}*

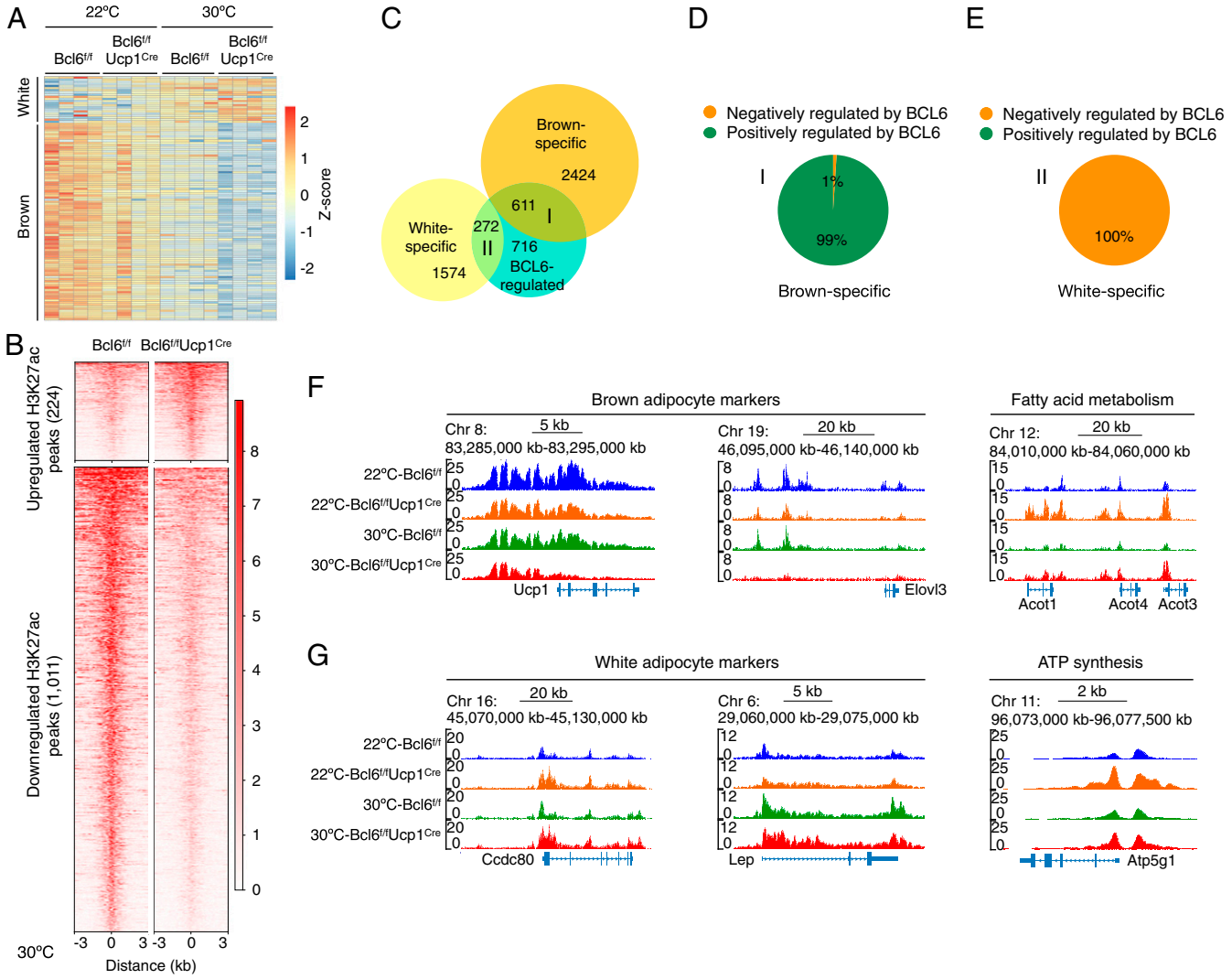

Fig. 5. BCL6 reinforces brown and opposes white adipocyte–specific enhancers to maintain cellular identity. (*A*) Heat map of nuclear encoded brown and white adipocyte–specific genes (BATLAS) in iBAT of *Bcl6*$^{f/f}$ and *Bcl6*$^{f/f}$*Ucp1*^{Cre} mice at 22 °C and 30 °C. The list of genes is provided in *SI Appendix*, Table S4. (*B*) Heat maps showing H3K27ac peaks that are up-regulated or down-regulated in iBAT of *Bcl6*$^{f/f}$*Ucp1*^{Cre} mice housed at 30 °C. H3K27ac peaks in heat maps represent an average of 3 biological replicates, and the amplitude of each peak center (±3 kb) is represented in color as indicated. (*C*) Venn diagram showing the overlap of BCL6-regulated enhancers at 30 °C with brown and white adipocyte–specific enhancers. The numbers indicate the number of enhancers in each field. (*D* and *E*) Pie charts showing the percentage of BCL6-regulated brown (*D*) and white (*E*) adipocyte–specific enhancers that are positively or negatively regulated by BCL6 at 30 °C. (*F* and *G*) Representative H3K27ac genome browser tracks for brown adipocyte–specific genes *Ucp1* and *Elovl3* (*F*), fatty acid metabolism genes *Acot1*, *Acot3*, and *Acot4* (*F*), white adipocyte–specific genes *Ccdc80* and *Lep* (*G*), and ATP synthesis gene *Atp5g1* (*G*). The effects of temperature and BCL6 are highlighted for each category. Data are presented as mean ± SEM.

mice, we postulated that BCL6 regulates brown adipocyte enhancers by both direct and indirect mechanisms. De novo sequence motif analysis revealed enrichment of the consensus binding motifs for hepatic leukemia factor (HLF) and BCL6 among the sites with increased H3K27 acetylation (Fig. 6*A*), whereas a nuclear receptor half site recognized by NR4A family members and estrogen-related receptors (ERRs) was enriched among the sites with reduced H3K27 acetylation in iBAT of *Bcl6*$^{f/f}$*Ucp1*^{Cre} mice (Fig. 6*B*). This suggested that while BCL6 directly represses a subset of enhancers and promoters, including those near *Atp5g1*, *Acot1*, *Bmf*, *Egln3*, and white adipocyte–specific genes *Lep*, *Ccdc80*, and *Nnat* (Figs. 2*D*, 3*F*, 4*D*, and 6*C*), it indirectly activates other regulatory sites, possibly by a mechanism involving ERRs, which are known to regulate fatty acid and oxidative metabolism in brown adipocytes (34, 35). Indeed, analysis of published ChIP-seq data for ERRα and ERRγ in BAT (36–39) revealed that the hypoacetylated H3K27 sites in iBAT of *Bcl6*$^{f/f}$*Ucp1*^{Cre} mice were highly enriched for ERRα and ERRγ binding (Fig. 6*D*). For example, we observed decreased H3K27 acetylation near *Ucp1* and genes involved in fatty acid oxidation, including *Slc27a2*, *Hadha*, *Hadhb*, and *Acaa2*, in iBAT of *Bcl6*$^{f/f}$*Ucp1*^{Cre} mice housed at 30 °C, which corresponded to regions of ERRα and ERRγ binding (Fig. 6*E*). These results suggest that BCL6 might regulate the expression of these key metabolic genes indirectly by promoting the activity of ERRs at their nearby enhancers and promoters.

To investigate this idea further, we analyzed the expression and recruitment of ERRs to their binding sites in dormant BAT. We observed that expression of the 3 ERR subtypes was similar in dormant iBAT of *Bcl6*$^{f/f}$ and *Bcl6*$^{f/f}$*Ucp1*^{Cre} mice (Fig. 6*F*). To determine if BCL6 modulated recruitment of ERRs to their respective binding sites near thermogenic genes, we performed ChIP-seq for ERRα in iBAT of *Bcl6*$^{f/f}$ and *Bcl6*$^{f/f}$*Ucp1*^{Cre} mice

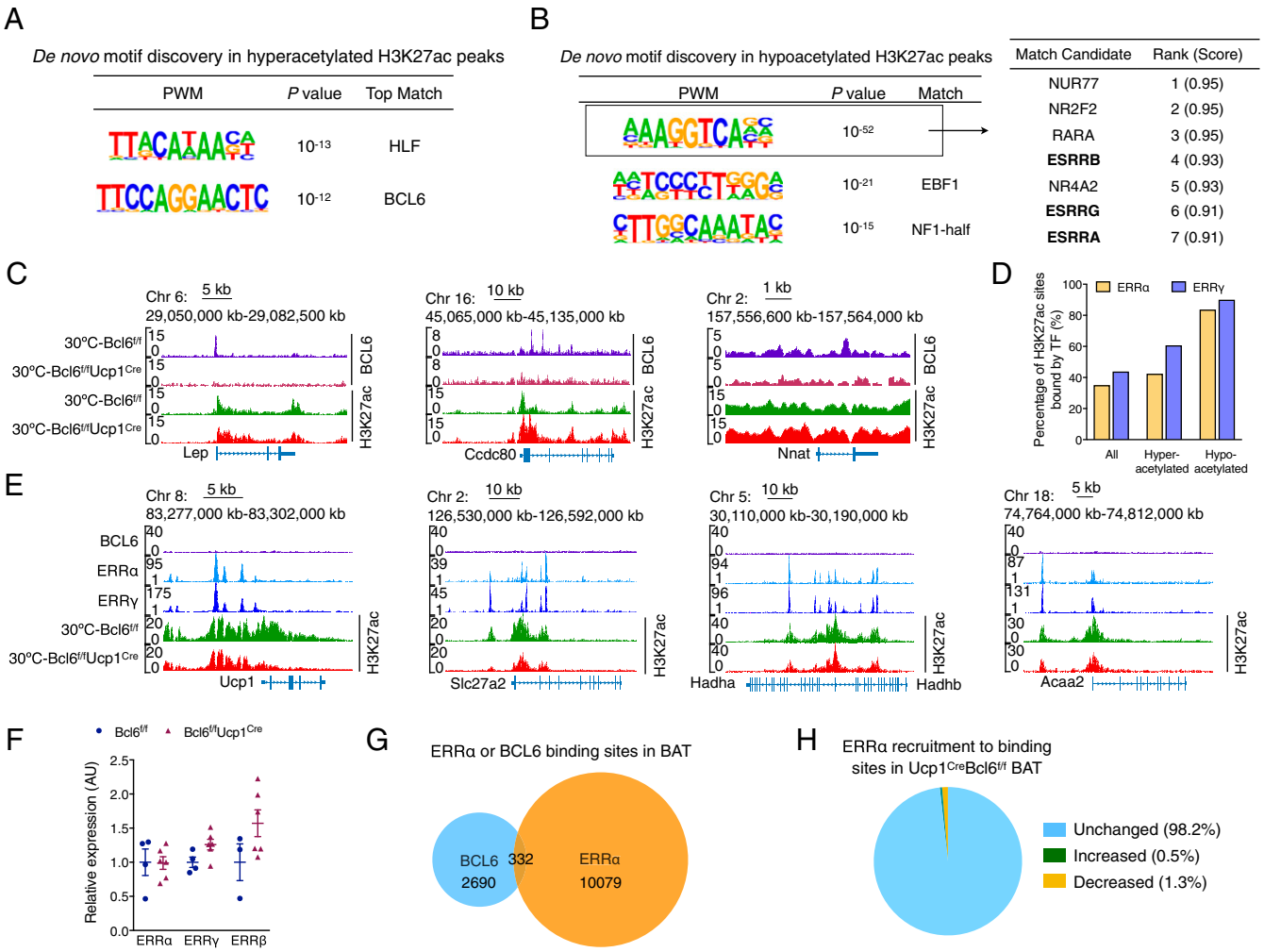

Fig. 6. BCL6 regulates brown adipocyte enhancers by direct and indirect mechanisms. (*A* and *B*) De novo sequence motif discovery at hyperacetylated (*A*) and hypoacetylated (*B*) H3K27 sites in iBAT of *Bcl6*$^{f/f}$*Ucp1*^{Cre} mice housed at 30 °C; PWM = position weight matrix. For the top enriched motif in *B*, a list of the top 7 matches from a database of known transcription factor binding site motifs and corresponding match scores are listed. (*C*) Genome browser tracks for visualization of the *Lep*, *Ccdc80*, and *Nnat* loci highlighting BCL6 and H3K27ac ChIP-seq data. (*D*) Percentage of H3K27 acetylation sites in iBAT (all sites or only sites that are hyperacetylated or hypoacetylated in *Bcl6*$^{f/f}$*Ucp1*^{Cre} mice at 30 °C) that are bound by ERRγ or ERRα. (*E*) Genome browser tracks for visualization of the *Ucp1*, *Slc27a2*, *Hadha*, *Hadhb*, and *Acaa2* loci highlighting BCL6, ERRα, ERRγ, and H3K27ac ChIP-seq data. (*F*) Quantitative RT-PCR measurement of *Esrra*, *Esrrg*, and *Esrrb* mRNA in iBAT of *Bcl6*$^{f/f}$ and *Bcl6*$^{f/f}$*Ucp1*^{Cre} mice housed at 30 °C ($n = 4$ to 6 per genotype). (*G*) Venn diagram showing the overlap between BCL6 and ERRα binding sites in iBAT at 30 °C. (*H*) ChIP-seq analysis of ERRα recruitment to binding sites in iBAT of *Bcl6*$^{f/f}$ and *Bcl6*$^{f/f}$*Ucp1*^{Cre} mice housed at 30 °C ($n = 4$ per genotype). Percentages of total binding sites with increased, decreased, or unchanged enrichment in *Bcl6*$^{f/f}$*Ucp1*^{Cre} mice are indicated. Data are presented as mean ± SEM.

housed at 30 °C. The cistromes of ERRα and BCL6 were largely nonoverlapping (Fig. 6*G*), indicating that they directly regulate distinct sets of genes. In addition, we found that recruitment of ERRα to the vast majority of its binding sites (98.2%) was not significantly different between the genotypes (Fig. 6*H*), suggesting that BCL6 does not regulate the recruitment of ERRα to its target genes. Although previous studies have implicated the coactivator protein PGC-1α and histone deacetylase HDAC3 in the transcriptional activation by ERRα (36, 40), the molecular and physiological phenotypes of mice lacking HDAC3 in brown adipocytes are distinct from those observed in *Bcl6*$^{f/f}$*Ucp1*^{Cre} mice. For example, loss of HDAC3 in brown adipocytes primarily affects genes involved in mitochondrial oxidative phosphorylation (36), metabolic pathways that are unaffected in brown adipocytes of *Bcl6*$^{f/f}$*Ucp1*^{Cre} mice. Thus, these findings suggest that BCL6 likely regulates the activity of ERRs at *Ucp1* and fatty acid oxidation genes by a distinct mechanism, which will need to be investigated in the future.

Discussion

Several characteristics set BCL6 apart from the "classical" transcriptional regulators of brown adipocyte commitment, differentiation, and activation, such as early B cell factor 2 (EBF2), peroxisome proliferator-activated receptor γ (PPARγ), ERRα/γ, CCAAT/enhancer binding protein (C/EBPβ), and IFN regulated factor 4 (IRF4) (41, 42). First, unlike transcription factors that act downstream of adrenergic stimuli, BCL6 operates in a parallel pathway, making it functionally more important during dormancy when sympathetic input into BAT is largely absent (Fig. 7). Second, unlike ERRα/γ, BCL6 is dispensable for expression of mitochondrial complexes involved in oxidative phosphorylation and electron transport but required for supporting uncoupled respiration and fatty acid oxidation in the mitochondria. Third, BCL6 directly binds to only a small number of genes linked to thermogenic metabolism, such as *Acot1* and *Atp5g1*, where it acts as a transcriptional repressor to sustain uncoupled respiration during dormancy. Fourth, BCL6 positively regulates many thermogenic genes by an indirect mechanism, possibly by

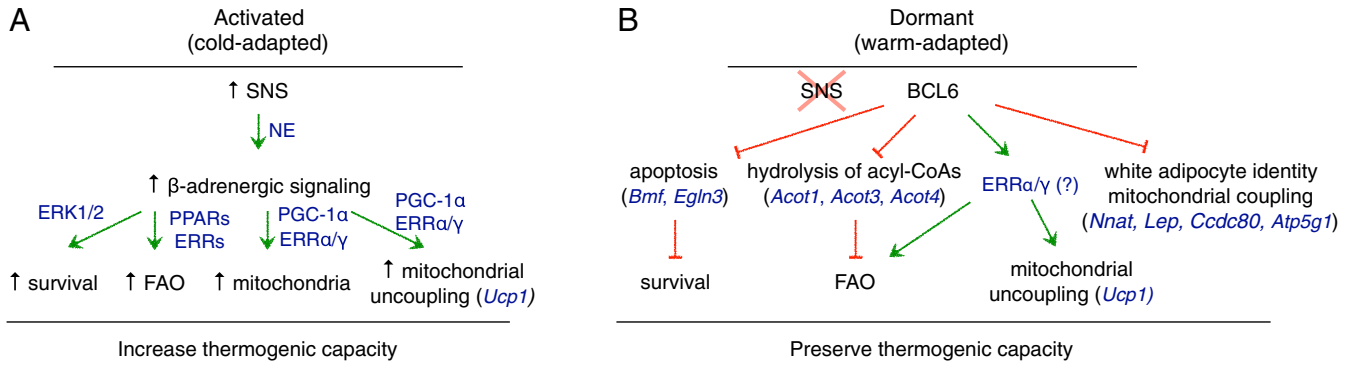

Fig. 7. A model for regulation of brown adipocyte dormancy by BCL6. (*A*) During adaptation to cold, norepinephrine (NE) released by the sympathetic nervous system (SNS) activates β-adrenergic signaling in brown adipocytes, which supports their survival and increases their thermogenic capacity. Survival is mediated by the action of ERK1/2, while fatty acid oxidation (FAO), mitochondrial biogenesis, and mitochondrial uncoupling (UCP1) are stimulated at the transcriptional level by peroxisome proliferator-activated receptors (PPARs), estrogen-related receptors (ERRs), and the coactivator protein PGC-1α. (*B*) In contrast, during adaptation to warmth, when sympathetic tone is minimal and brown adipocytes become dormant, BCL6 reinforces survival and preserves thermogenic capacity. BCL6 promotes survival by repressing proapoptotic genes, such as *Bmf* and *Egln3*, and maintains reserve thermogenic capacity by repressing genes involved in hydrolysis of acyl-CoAs (*Acot1, Acot3, Acot4*) and mitochondrial coupling (*Atp5g1*), as well as white adipocyte–specific genes (*Nnat, Lep, Ccdc80*) and potentially by stimulating the activity of ERRs to promote expression of genes involved in FAO and uncoupled respiration (*Ucp1*).

activating ERRs. The potential regulation of ERR transcriptional activity by BCL6 is intriguing because it might represent a point of convergence with the adrenergic signaling pathway, which is known to induce expression and activity of ERRs (34). In this scenario, BCL6 might be important for maintaining basal activity of ERRs during dormancy, whereas full activation of ERRα/γ by adrenergic stimuli is necessary for adaptation to environmental cold. In support of this model, the molecular, histological, and physiological phenotypes of mice lacking ERRα/γ or ERRγ in their brown adipocytes partially overlap with those observed in dormant BAT of $Bcl6^{f/f}Ucp1^{Cre}$ mice (37, 43). Although these data suggest convergence of BCL6 and ERRs in expression of thermogenic genes in dormant brown adipocytes, the precise mechanisms will require additional investigations in the future.

During adaptation to cold, BAT cellularity increases to support the higher demand for thermogenesis. This is due to the positive effect of adrenergic signaling on proliferation of brown adipocyte precursors and survival of differentiated brown adipocytes (28, 44). However, since the rate of apoptosis is low in dormant BAT of wild-type mice (45, 46), additional factors likely promote survival of brown adipocytes in the absence of adrenergic signals. Three distinct lines of evidence suggest that BCL6 is a critical factor that enhances survival of brown adipocytes when adrenergic input into this tissue is low. First, genetic deficiency of *Bcl6* increased apoptosis of brown adipocytes, leading to reduction of BAT cellularity in thermoneutral mice. Second, loss of BCL6 increased expression of genes involved in promotion of apoptosis. Third, BCL6 directly bound to a subset of proapoptotic genes, including *Bmf* and *Egln3*, resulting in their repression in control animals. Thus, in the absence of adrenergic signals, BCL6 acts in a cell-autonomous manner to promote survival of brown adipocytes.

The chromatin state of differentiated cells is known to be highly stable and can be used to distinguish one differentiated cell type from another (47). For example, in response to changes in environmental temperature, brown adipocytes dramatically alter their morphology and gene expression but maintain a relatively stable chromatin state (10). Although this epigenetic state of brown adipocytes is established during differentiation in an EBF2-dependent manner (48), it was not known what factors might be involved in its stable maintenance across different thermal conditions. The data presented here demonstrate that BCL6 contributes to the maintenance of the stable epigenetic landscape of brown adipocytes. BCL6 accomplishes this by simultaneously reinforcing brown-specific enhancers while opposing white-specific enhancers in dormant BAT. Since ∼17% of the active enhancers regulated by BCL6 were white specific, it suggests that BCL6, in part, maintains the cellular identity of brown adipocytes by repressing alternative cellular fates. In support of this hypothesis, profiling of genes comprising the BATLAS, which can be used to assess enrichment of white or brown adipocytes in adipose tissues (32), revealed a dramatic shift in the cellular identity of iBAT of $Bcl6^{f/f}Ucp1^{Cre}$ mice. In particular, we found that expression of white adipocytes markers was increased, whereas expression of brown adipocyte selective genes was decreased in iBAT of $Bcl6^{f/f}Ucp1^{Cre}$ mice. Together, these findings demonstrate that the transcriptional repressor BCL6 is critically important for the maintenance of cellular identity of brown adipocytes but not for their differentiation or thermogenic activation by adrenergic stimuli.

Previous studies have suggested that UCP1 not only provides a defense against environmental cold (49) but also contributes to diet-induced thermogenesis to mitigate the deleterious effects of obesogenic diets (27). This antiobesity effect of UCP1 was originally uncovered by housing $Ucp1^{-/-}$ mice at thermoneutrality and challenging them with a high-fat diet. Since thermoneutral mice do not engage in cold-induced thermogenesis, the increased weight gain observed in $Ucp1^{-/-}$ mice was attributed to increased metabolic efficiency stemming from the absence of diet-induced thermogenesis (27). In contrast, we found that while BCL6 was essential for maintenance of thermogenic fitness during transition from thermoneutrality to cold, it was dispensable for diet-induced thermogenesis in thermoneutral mice. Because a similar disconnect between cold- and diet-induced thermogenesis has been observed in other mouse models, including mice lacking *Prdm16*, *ERRα/γ*, *Cpt2*, and *Hdac3* in their brown adipocytes (36, 43, 50–52), it suggests that increased metabolic efficiency and predisposition to diet-induced obesity might be a unique feature of $Ucp1^{-/-}$ mice. In this regard, recent studies demonstrate that in addition to the absence of UCP1, expression and activity of the mitochondrial respiratory chain are severely reduced in BAT of $Ucp1^{-/-}$ mice (53, 54). Together, these findings suggest that the metabolic phenotypes observed in $Ucp1^{-/-}$ mice might not accurately reflect the putative functions of BAT in diet-induced thermogenesis, an issue that remains controversial in the literature (55). Because there is immense clinical interest in therapeutic targeting of BAT for the treatment of obesity and metabolic diseases (56–59), additional studies will be necessary to validate the functions of BAT in diet-induced thermogenesis in both mice and humans.

Animal Studies

All experiments involving mice were conducted under an approved Institutional Animal Care and Use Committee (IACUC) protocol at University of California, San Francisco (UCSF).

ACKNOWLEDGMENTS. We thank members of the A.C. laboratory for discussions and comments and X. Cui for assistance with mouse husbandry. The authors' work was supported by grants from NIH (DK094641 and DK101064, to A.C.) and AHA Predoctoral Fellowship (18PRE34080250 and 16PRE26960008, to V.I.K.). Histology support was provided by the UCSF Liver Center (NIH P30DK026743).

1. B. Cannon, J. Nedergaard, Brown adipose tissue: Function and physiological significance. *Physiol. Rev.* **84**, 277–359 (2004).
2. B. B. Lowell, B. M. Spiegelman, Towards a molecular understanding of adaptive thermogenesis. *Nature* **404**, 652–660 (2000).
3. M. Harms, P. Seale, Brown and beige fat: Development, function and therapeutic potential. *Nat. Med.* **19**, 1252–1263 (2013).
4. B. Cannon, J. Nedergaard, Nonshivering thermogenesis and its adequate measurement in metabolic studies. *J. Exp. Biol.* **214**, 242–253 (2011).
5. A. M. Cypess *et al*., Identification and importance of brown adipose tissue in adult humans. *N. Engl. J. Med.* **360**, 1509–1517 (2009).
6. W. D. van Marken Lichtenbelt *et al*., Cold-activated brown adipose tissue in healthy men. *N. Engl. J. Med.* **360**, 1500–1508 (2009).
7. K. A. Virtanen *et al*., Functional brown adipose tissue in healthy adults. *N. Engl. J. Med.* **360**, 1518–1525 (2009).
8. H. A. Daanen, W. D. Van Marken Lichtenbelt, Human whole body cold adaptation. *Temperature (Austin)* **3**, 104–118 (2016).
9. J. M. Heaton, The distribution of brown adipose tissue in the human. *J. Anat.* **112**, 35–39 (1972).
10. H. C. Roh *et al*., Warming induces significant reprogramming of beige, but not brown, adipocyte cellular identity. *Cell Metab.* **27**, 1121–1137.e5 (2018).
11. J. Sanchez-Gurmaches, C. M. Hung, D. A. Guertin, Emerging complexities in adipocyte origins and identity. *Trends Cell Biol.* **26**, 313–326 (2016).
12. A. L. Dent, A. L. Shaffer, X. Yu, D. Allman, L. M. Staudt, Control of inflammation, cytokine expression, and germinal center formation by BCL-6. *Science* **276**, 589–592 (1997).
13. B. H. Ye *et al*., The BCL-6 proto-oncogene controls germinal-centre formation and Th2-type inflammation. *Nat. Genet.* **16**, 161–170 (1997).
14. R. I. Nurieva *et al*., Bcl6 mediates the development of T follicular helper cells. *Science* **325**, 1001–1005 (2009).
15. R. J. Johnston *et al*., Bcl6 and Blimp-1 are reciprocal and antagonistic regulators of T follicular helper cell differentiation. *Science* **325**, 1006–1010 (2009).
16. C. H. Lee *et al*., Transcriptional repression of atherogenic inflammation: Modulation by PPARdelta. *Science* **302**, 453–457 (2003).
17. G. D. Barish *et al*., Bcl-6 and NF-kappaB cistromes mediate opposing regulation of the innate immune response. *Genes Dev.* **24**, 2760–2765 (2010).
18. A. L. Basse *et al*., Global gene expression profiling of brown to white adipose tissue transformation in sheep reveals novel transcriptional components linked to adipose remodeling. *BMC Genomics* **16**, 215 (2015).
19. C. R. LaPensee, G. Lin, A. L. Dent, J. Schwartz, Deficiency of the transcriptional repressor B cell lymphoma 6 (Bcl6) is accompanied by dysregulated lipid metabolism. *PLoS One* **9**, e97090 (2014).
20. X. Hu *et al*., Identification of zinc finger protein Bcl6 as a novel regulator of early adipose commitment. *Open Biol.* **6**, 160065 (2016).
21. M. D. Senagolage *et al*., Loss of transcriptional repression by BCL6 confers insulin sensitivity in the setting of obesity. *Cell Rep.* **25**, 3283–3298.e6 (2018).
22. M. A. Sommars *et al*., Dynamic repression by BCL6 controls the genome-wide liver response to fasting and steatosis. *eLife* **8**, e43922 (2019).
23. J. G. Granneman, M. Burnazi, Z. Zhu, L. A. Schwamb, White adipose tissue contributes to UCP1-independent thermogenesis. *Am. J. Physiol. Endocrinol. Metab.* **285**, E1230–E1236 (2003).
24. V. Golozoubova, B. Cannon, J. Nedergaard, UCP1 is essential for adaptive adrenergic nonshivering thermogenesis. *Am. J. Physiol. Endocrinol. Metab.* **291**, E350–E357 (2006).
25. J. Houstek, U. Andersson, P. Tvrdik, J. Nedergaard, B. Cannon, The expression of subunit c correlates with and thus may limit the biosynthesis of the mitochondrial F0F1-ATPase in brown adipose tissue. *J. Biol. Chem.* **270**, 7689–7694 (1995).
26. T. V. Kramarova *et al*., Mitochondrial ATP synthase levels in brown adipose tissue are governed by the c-Fo subunit P1 isoform. *FASEB J.* **22**, 55–63 (2008).
27. H. M. Feldmann, V. Golozoubova, B. Cannon, J. Nedergaard, UCP1 ablation induces obesity and abolishes diet-induced thermogenesis in mice exempt from thermal stress by living at thermoneutrality. *Cell Metab.* **9**, 203–209 (2009).
28. J. M. Lindquist, S. Rehnmark, Ambient temperature regulation of apoptosis in brown adipose tissue. Erk1/2 promotes norepinephrine-dependent cell survival. *J. Biol. Chem.* **273**, 30147–30156 (1998).
29. J. Nedergaard, Y. Wang, B. Cannon, Cell proliferation and apoptosis inhibition: Essential processes for recruitment of the full thermogenic capacity of brown adipose tissue. *Biochim. Biophys. Acta Mol. Cell Biol. Lipids* **1864**, 51–58, (2019).
30. V. Tillander, S. E. H. Alexson, D. E. Cohen, Deactivating fatty acids: Acyl-CoA thioesterase-mediated control of lipid metabolism. *Trends Endocrinol. Metab.* **28**, 473–484 (2017).
31. K. Okada *et al*., Thioesterase superfamily member 1 suppresses cold thermogenesis by limiting the oxidation of lipid droplet-derived fatty acids in brown adipose tissue. *Mol. Metab.* **5**, 340–351 (2016).
32. A. Perdikari *et al*., BATLAS: Deconvoluting brown adipose tissue. *Cell Rep.* **25**, 784–797.e4 (2018).
33. H. Roh, E. Rosen, Data from "Warming induces significant reprogramming of beige, but not brown, adipocyte cellular identity." Gene Expression Omnibus. https://www.ncbi.nlm.nih.gov//geo/query/acc.cgi?acc=GSE108077. Accessed 2 May 2018.
34. V. Giguere, Transcriptional control of energy homeostasis by the estrogen-related receptors. *Endocr. Rev.* **29**, 677–696 (2008).
35. J. A. Villena, A. Kralli, ERRalpha: A metabolic function for the oldest orphan. *Trends Endocrinol. Metab.* **19**, 269–276 (2008).
36. M. J. Emmett *et al*., Histone deacetylase 3 prepares brown adipose tissue for acute thermogenic challenge. *Nature* **546**, 544–548 (2017).
37. M. Ahmadian *et al*., ERRgamma preserves brown fat innate thermogenic activity. *Cell Rep.* **22**, 2849–2859 (2018).
38. M. J. Emmett, H. Lim, K. Won, M. A. Lazar, Data from "Histone Deacetylase 3 Prepares Brown Adipose Tissue For Acute Thermogenic Challenge." Gene Expression Omnibus. https://www.ncbi.nlm.nih.gov/geo/query/acc.cgi?acc=GSE83927. Accessed 28 October 2018.
39. M. Ahmadian, R. M. Evans, Data from "The nuclear receptor ERR? maintains innate brown fat thermogenic capacity." Sequence Read Archive. https://trace.ncbi.nlm.nih.gov/Traces/sra/?study=SRP063705. Accessed 28 October 2018.
40. S. N. Schreiber *et al*., The estrogen-related receptor alpha (ERRalpha) functions in PPARgamma coactivator 1alpha (PGC-1alpha)-induced mitochondrial biogenesis. *Proc. Natl. Acad. Sci. U.S.A.* **101**, 6472–6477 (2004).
41. W. Wang, P. Seale, Control of brown and beige fat development. *Nat. Rev. Mol. Cell Biol.* **17**, 691–702 (2016).
42. A. Loft, I. Forss, S. Mandrup, Genome-wide insights into the development and function of thermogenic adipocytes. *Trends Endocrinol. Metab.* **28**, 104–120 (2017).
43. E. L. Brown *et al*., Estrogen-related receptors mediate the adaptive response of brown adipose tissue to adrenergic stimulation. *iScience* **2**, 221–237 (2018).
44. Y. H. Lee, A. P. Petkova, A. A. Konkar, J. G. Granneman, Cellular origins of cold-induced brown adipocytes in adult mice. *FASEB J.* **29**, 286–299 (2015).
45. B. Hellman, C. Hellerstrom, Cell renewal in the white and brown fat tissue of the rat. *Acta Pathol. Microbiol. Scand.* **51**, 347–353 (1961).
46. P. Kotzbeck *et al*., Brown adipose tissue whitening leads to brown adipocyte death and adipose tissue inflammation. *J. Lipid Res.* **59**, 784–794 (2018).
47. R. Feil, M. F. Fraga, Epigenetics and the environment: Emerging patterns and implications. *Nat. Rev. Genet.* **13**, 97–109 (2012).
48. S. N. Shapira *et al*., EBF2 transcriptionally regulates brown adipogenesis via the histone reader DPF3 and the BAF chromatin remodeling complex. *Genes Dev.* **31**, 660–673 (2017).
49. S. Enerback *et al*., Mice lacking mitochondrial uncoupling protein are cold-sensitive but not obese. *Nature* **387**, 90–94 (1997).
50. M. J. Harms *et al*., Prdm16 is required for the maintenance of brown adipocyte identity and function in adult mice. *Cell Metab.* **19**, 593–604 (2014).
51. J. Lee, J. Choi, S. Aja, S. Scafidi, M. J. Wolfgang, Loss of adipose fatty acid oxidation does not potentiate obesity at thermoneutrality. *Cell Rep.* **14**, 1308–1316 (2016).
52. J. Lee, J. M. Ellis, M. J. Wolfgang, Adipose fatty acid oxidation is required for thermogenesis and potentiates oxidative stress-induced inflammation. *Cell Rep.* **10**, 266–279 (2015).
53. J. I. Odegaard *et al*., Perinatal licensing of thermogenesis by IL-33 and ST2. *Cell* **166**, 841–854 (2016).
54. L. Kazak *et al*., UCP1 deficiency causes brown fat respiratory chain depletion and sensitizes mitochondria to calcium overload-induced dysfunction. *Proc. Natl. Acad. Sci. U.S.A.* **114**, 7981–7986 (2017).
55. L. P. Kozak, Brown fat and the myth of diet-induced thermogenesis. *Cell Metab.* **11**, 263–267 (2010).
56. S. Kajimura, B. M. Spiegelman, P. Seale, Brown and beige fat: Physiological roles beyond heat generation. *Cell Metab.* **22**, 546–559 (2015).
57. Y. H. Tseng, A. M. Cypess, C. R. Kahn, Cellular bioenergetics as a target for obesity therapy. *Nat. Rev. Drug Discov.* **9**, 465–482 (2010).
58. M. J. Vosselman, W. D. van Marken Lichtenbelt, P. Schrauwen, Energy dissipation in brown adipose tissue: From mice to men. *Mol. Cell. Endocrinol.* **379**, 43–50 (2013).
59. S. Enerback, Human brown adipose tissue. *Cell Metab.* **11**, 248–252 (2010).